QUANTUM SIMULATION

A scalable realization of local U(1) gauge invariance in cold atomic mixtures

Alexander Mil[1]*, Torsten V. Zache[2], Apoorva Hegde[1], Andy Xia[1], Rohit P. Bhatt[1], Markus K. Oberthaler[1], Philipp Hauke[1,2,3], Jürgen Berges[2], Fred Jendrzejewski[1]

In the fundamental laws of physics, gauge fields mediate the interaction between charged particles. An example is the quantum theory of electrons interacting with the electromagnetic field, based on U(1) gauge symmetry. Solving such gauge theories is in general a hard problem for classical computational techniques. Although quantum computers suggest a way forward, large-scale digital quantum devices for complex simulations are difficult to build. We propose a scalable analog quantum simulator of a U(1) gauge theory in one spatial dimension. Using interspecies spin-changing collisions in an atomic mixture, we achieve gauge-invariant interactions between matter and gauge fields with spin- and species-independent trapping potentials. We experimentally realize the elementary building block as a key step toward a platform for quantum simulations of continuous gauge theories.

Gauge symmetries are a cornerstone of our fundamental description of quantum physics as encoded in the standard model of particle physics. The presence of a gauge symmetry implies a concerted dynamics of matter and gauge fields that is subject to local symmetry constraints at each point in space and time (*1*). To uncover the complex dynamical properties of such highly constrained quantum many-body systems, enormous computational resources are required. This difficulty is stimulating great efforts to quantum simulate these systems, i.e., to solve their dynamics using highly controlled experimental setups with synthetic quantum systems (*2*–*4*). First experimental breakthroughs have used quantum-computer algorithms that implement gauge invariance exactly, but which are either limited to one spatial dimension (*5*, *6*), restrict the dynamics of the gauge fields (*7*, *8*), or require classical preprocessing resources that scale exponentially with system size (*9*). Recently, the dynamics of a discrete Z_2 gauge theory in a minimal model has been realized based on Floquet engineering (*10*–*12*). Despite these advances, the faithful realization of large-scale quantum simulators describing the continuum behavior of gauge theories remains highly challenging.

Our aim is the development of a scalable and highly tunable platform for a continuous U(1) gauge theory, such as realized in quantum electrodynamics. In the past years, ultracold atoms have become a well-established system for mimicking condensed-matter models with static electric and magnetic fields (*13*) and even dynamical background fields for moving particles (*14*–*16*). These systems possess global U(1) symmetries related to the conservation of total magnetization and atom number (*17*). However, a gauge theory is based on a local symmetry, which we enforce here through spin-changing collisions in atomic mixtures. This promising mechanism to protect gauge invariance has been put forward in various proposals (*18*–*21*) but not yet demonstrated experimentally. We demonstrate the engineering of an elementary building block in a mixture of bosonic atoms, demonstrate its high tunability, and verify its faithful representation of the desired model.

We further propose an extended implementation scheme in an optical lattice, where each lattice well constitutes an elementary building block that contains both matter and gauge fields. Repetitions of this elementary unit can be connected using Raman-assisted tunneling (*22*). Gauge and matter fields are spatially arranged in such a way that the spin-changing collisions occur within single-lattice wells, in contrast to previous proposals (*18*–*21*) where the gauge and matter fields were spatially separated and spin-changing collisions had to be accompanied by hopping across different sites of the optical lattice.

We specify our proposal for a one-dimensional gauge theory on a spatial lattice, as visualized

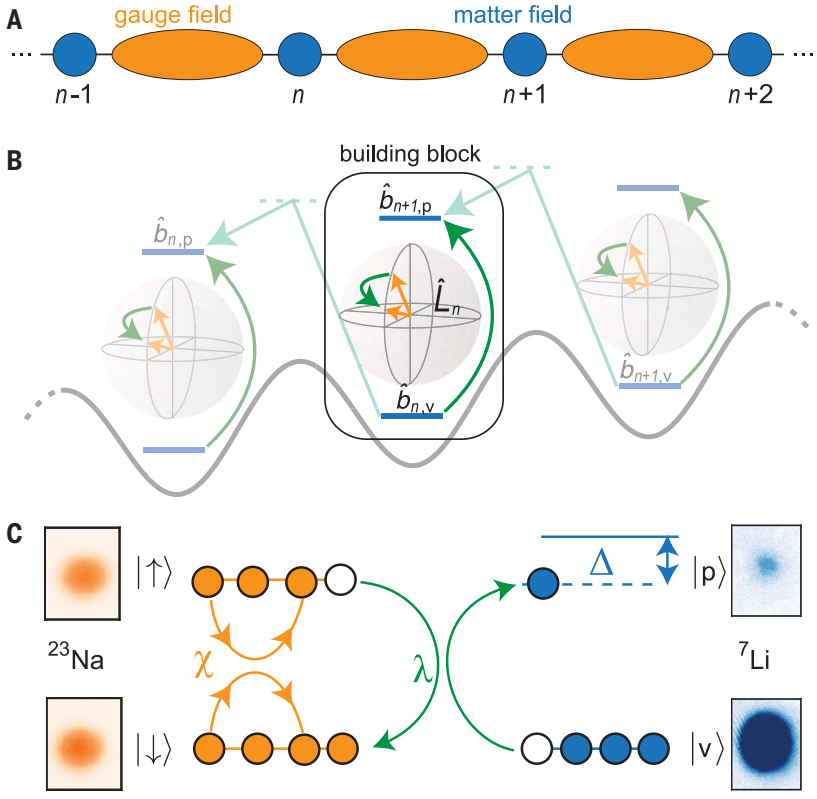

Fig. 1. Engineering a gauge theory. (**A**) Structure of a lattice gauge theory. Matter fields reside on sites and gauge fields on the links in between. (**B**) Proposed implementation of the extended system. Individual building blocks consist of long spins (representing gauge fields) and matter states, which are confined within the same well and whose interaction constitutes a local U(1) symmetry. An array of building blocks in an optical lattice is connected via Raman-assisted tunneling. (**C**) Experimental realization of the elementary building block with bosonic gauge (sodium) and matter (lithium) fields. The gauge-invariant interaction is realized by heteronuclear spin-changing collisions.

[1]Kirchhoff-Institut für Physik, Heidelberg University, Im Neuenheimer Feld 227, 69120 Heidelberg, Germany. [2]Institut für Theoretische Physik, Heidelberg University, Philosophenweg 16, 69120 Heidelberg, Germany. [3]INO-CNR BEC Center and Department of Physics, University of Trento, Via Sommarive 14, I-38123 Trento, Italy.
*Corresponding author. Email: block@synqs.org

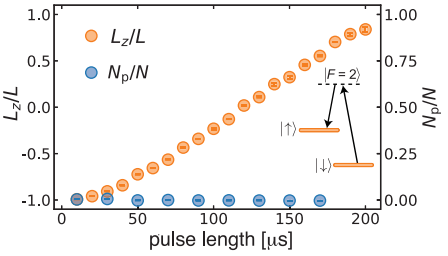

Fig. 2. Tunability of the initial conditions. The normalized spin z-component L_z/L of ^{23}Na atoms as a function of the preparation pulse length, which shows that the gauge field can be tuned experimentally over the entire possible range. Simultaneously, the particle number N_p/N of ^{7}Li is kept in the vacuum state. The inset shows a sketch of the experimental protocol used for tuning the initial conditions.

in Fig. 1A. Charged matter fields reside on the lattice sites n, with gauge fields on the links in between the sites (*23*). We consider two-component matter fields labeled "p" and "v", which are described by the operators $(\hat{b}_{n,\mathrm{p}}, \hat{b}_{n,\mathrm{v}})$. To realize the gauge fields with the atomic system, we use the quantum link formulation (*24*–*26*), where the gauge fields are replaced by quantum mechanical spins $\hat{\mathbf{L}}_n = (\hat{L}_{x,n}, \hat{L}_{y,n}, \hat{L}_{z,n})$, labeling link operators by the index of the site to the left. In this formulation, the spin z-component $\hat{L}_{n,z}$ can be identified with a discrete "electric" field. We recover the continuous gauge fields of the original quantum field theory in a controlled way by working in the limit of long spins (*20*).

Physically, this system of charged matter and gauge fields can be realized in a mixture of two atomic Bose–Einstein condensates (BECs) with two internal components each (in our experiment, we use ^{7}Li and ^{23}Na). An extended system can be obtained by use of an optical lattice. In our scheme, we abandon the one-to-one correspondence between the sites of the simulated lattice gauge theory and the sites of the optical-lattice simulator. This correspondence characterized previous proposals and necessitated physically placing the gauge fields in-between matter sites (*18*–*21*). Instead, as illustrated in Fig. 1B, here one site of the physical lattice hosts two matter components, each taken from one adjacent site ($\hat{b}_{n+1,\mathrm{p}}$ and $\hat{b}_{n,\mathrm{v}}$), as well as the link ($\hat{\mathbf{L}}_n$).

The enhanced physical overlap in this configuration decisively improved time scales of the spin-changing collisions, which until now were a major limiting factor for experimental implementations. Moreover, a single well of the optical lattice already contains the essential processes between matter and gauge fields and thus represents an elementary building block of the lattice gauge theory. These building blocks can be coupled by Raman-assisted tunneling of the matter fields [see supplementary materials (SM)].

The Hamiltonian $\hat{H} = \sum[\hat{H}_n + \hbar\Omega(\hat{b}^{\dagger}_{n,\mathrm{p}}\hat{b}_{n,\mathrm{v}} + \hat{b}^{\dagger}_{n,\mathrm{v}}\hat{b}_{n,\mathrm{p}})]$ of the extended system can thus be decomposed into the elementary building-block Hamiltonian $\hat{H}_n$ and the Raman-assisted tunneling (with Raman frequency ~Ω). Here, $\hat{H}_n$ reads (writing $\hat{b}_{\mathrm{p}} \equiv \hat{b}_{n+1,\mathrm{p}}$, $\hat{b}_{\mathrm{v}} \equiv \hat{b}_{n,\mathrm{v}}$, and $\hat{\mathbf{L}} \equiv \hat{\mathbf{L}}_n$)

$$\hat{H}_n/\hbar = \chi\hat{L}_z^2 + \frac{\Delta}{2}(\hat{b}^{\dagger}_{\mathrm{p}}\hat{b}_{\mathrm{p}} - \hat{b}^{\dagger}_{\mathrm{v}}\hat{b}_{\mathrm{v}}) + \lambda(\hat{b}^{\dagger}_{\mathrm{p}}\hat{L}_-\hat{b}_{\mathrm{v}} + \hat{b}^{\dagger}_{\mathrm{v}}\hat{L}_+\hat{b}_{\mathrm{p}}) \quad (1)$$

where $\hat{L}_+ = \hat{L}_x + i\hat{L}_y$ and $\hat{L}_- = \hat{L}_x - i\hat{L}_y$. The first term on the right-hand side of Eq. 1, which is proportional to the parameter χ, describes the energy of the gauge field, and the second term, ~Δ, sets the energy difference between the two matter components. The last term, ~λ, describes the U(1) invariant coupling between matter and gauge fields, which is essential to retain the local U(1) gauge symmetry of the Hamiltonian $\hat{H}$ (see SM for more details).

We implemented the elementary building block Hamiltonian $\hat{H}_n$ with a mixture of $2L \sim 300 \times 10^3$ sodium and $N \sim 50 \times 10^3$ lithium atoms as sketched in Fig. 1C (see SM for details). Both species were kept in an optical dipole trap such that the external trapping potential is spin insensitive for both species. An external magnetic bias field of $B \approx 2$G suppressed any spin change energetically, such that only the two Zeeman levels, $m_F = 0$ and 1, of the $F = 1$ hyperfine ground state manifolds were populated during the experiment. The ^{23}Na states are labeled as $|\uparrow\rangle = |m_F = 0\rangle$ and $|\downarrow\rangle = |m_F = 1\rangle$, on which the spin operator $\hat{\mathbf{L}}$ associated to the gauge field acts. The first term of Eq. 1 is then identified with the one-axis twisting Hamiltonian (*27*, *28*). We label the ^{7}Li states as "particle" $|\mathrm{p}\rangle = |m_F = 0\rangle$ and "vacuum" $|\mathrm{v}\rangle = |m_F = 1\rangle$, in accordance with the matter field operators $\hat{b}_{\mathrm{p}}$ and $\hat{b}_{\mathrm{v}}$. With this identification, the second term arises from energy shifts due to the external magnetic field and density interactions. Finally, the term ~λ is physically implemented by heteronuclear spin-changing interactions (*29*).

The resulting setup is highly tunable, as we demonstrated experimentally on the building block. We achieved tunability of the gauge field through a two-pulse Rabi coupling of the Na atoms between $|\downarrow\rangle$ and $|\uparrow\rangle$ using an intermediate $|F = 2\rangle$ state, which yields a desired value of $L_z/L = (N_\uparrow - N_\downarrow)/(N_\uparrow + N_\downarrow)$ (Fig. 2). At the same time, we kept the ^{7}Li atoms in $|\mathrm{v}\rangle$, corresponding to the initial vacuum of the matter sector at $\Delta \to \infty$, with $\lesssim$1% detected in $|\mathrm{p}\rangle$ (Fig. 2).

When the gauge-invariant coupling was turned off by removing the Na atoms from the trap, we observed no dynamics in the matter sector beyond the detection noise. By contrast, once the gauge field was present, the matter sector clearly underwent a transfer from $|\mathrm{v}\rangle$ to $|\mathrm{p}\rangle$ for proper initial conditions, as illustrated in Fig. 3A for an initialization to $L_z/L = -0.188$ at a magnetic field of $B_{\mathrm{A}} = 2.118(2)$G (*30*). This observation demonstrated the controlled operation of heteronuclear spin-changing collisions implementing the gauge-invariant dynamics in the experiment.

To quantify our observations, we extracted the ratio N_{p}/N, with $N = N_{\mathrm{p}} + N_{\mathrm{v}}$, as a function of time as presented in Fig. 3B. We observed nonzero N_{p}/N, describing "particle production," on a time scale of a few tens of milliseconds, with up to 6% of the total N being transferred to $|\mathrm{p}\rangle$. This value is consistent with our expectations from conservation of the initial energy $E_0/\hbar = \chi L_z^2 - \Delta N_{\mathrm{v}}/2$, from which we estimated a maximum amplitude on the order of a few percent. Owing to the much larger ^{23}Na condensate, the expected corresponding change in L_z/L is ~2%, which is currently not detectable with our imaging routine (see SM for details). Coherent oscillations in N_{p}/N were seen to persist for about 100ms.

We display N_{p}/N over the entire range of initial L_z in Fig. 4, keeping a fixed time of 30ms. The upper panel (A) corresponds to the same experimental setting as in Fig. 3. A clear resonance for particle production can be seen around $L_z/L \simeq -0.5$, approximately captured by the resonance condition $2\chi L_z \sim \Delta$ (see SM

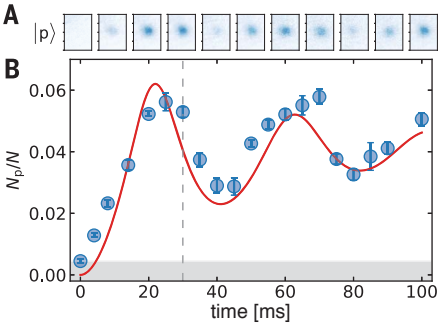

Fig. 3. Dynamics of particle production. (**A**) The number density distribution in state $|\mathrm{p}\rangle$ as a function of time for $L_z/L = -0.188$. (**B**) The corresponding particle number N_{p}/N. The blue circles give the experimental values with bars indicating the statistical error on the mean. The red curve is the theoretical mean-field prediction of Hamiltonian (Eq. 1) with parameters determined from a fit of the data in Fig. 4A and phenomenological damping. The shaded area indicates the experimental noise floor. The dashed line marks the time of 30 ms as it is used for the experimental sequence generating the data in Fig. 4.

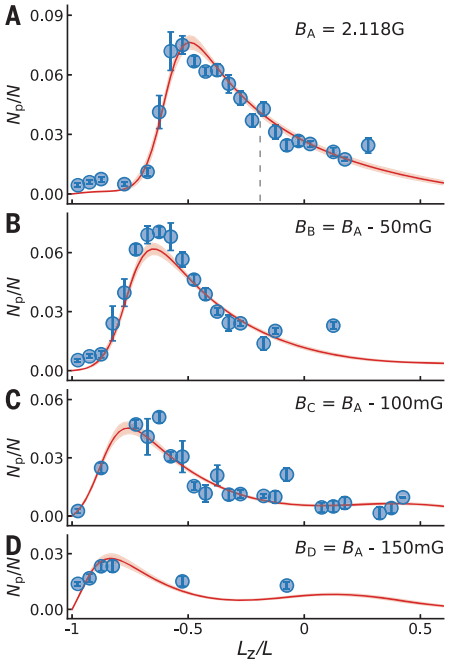

Fig. 4. Resonant particle production. (**A** to **D**) The number of produced particles as a function of initially prepared L_z/L after 30 ms for different-bias magnetic fields. Blue circles are experimental values with bars indicating the statistical error on the mean. The red curve in (A) arises from the theoretical model using the best estimate values of χ, λ, Δ_0, and Δ_L. The remaining curves in (B) to (D) are computed using the same parameters, including Δ_B. The shaded area indicates confidence intervals of the fit from bootstrap resampling. The dashed line in (A) indicates the L_z/L value corresponding to the time evolution shown in Fig. 3.

for details). The asymmetry of the resonance is a clear manifestation of the nonlinearity of the dynamics. As we reduced the magnetic field B, presented in Fig. 4, B to D, we observed a shift of the resonant particle production together with a reduction in amplitude, which continued to be qualitatively captured by the resonance condition $2\chi L_z \sim \Delta$. The maximal amplitude of the particle production was necessarily reduced by the conservation of total magnetization as the resonant peak was pushed closer to $L_z/L = -1$. For fields that were smaller than $B_{\min} \approx 1.96$G, the matter and gauge field dynamics became too off-resonant, and particle production was not observed any longer.

We compare the experimental results to the mean-field predictions of Hamiltonian (Eq. 1) for chosen χ, λ, and $\Delta(L_z, B) = \Delta_0 + \Delta_L L_z/L + \Delta_B(B - B_A)/B_A$ (see SM for the origin of the dependence on the magnetic field B and the initial spin L_z). A first-principle calculation of these model parameters, using only the experimental input of our setup, yielded $\chi^{\mathrm{th}}/2\pi \approx 14.92$mHz, $\lambda^{\mathrm{th}}/2\pi \approx 42.3\mu$Hz, $\Delta_0^{\mathrm{th}}/2\pi \approx -77$Hz, $\Delta_L^{\mathrm{th}}/2\pi \approx 4.474$kHz, and $\Delta_B^{\mathrm{th}}/2\pi \approx -1.669$kHz. These values were obtained by neglecting any residual spatial dynamics (*31*) of the atomic clouds within the trapping potential, which renormalized the model parameters. Moreover, the mean-field approximation was not able to capture the decoherence observed in Fig. 3 at later times. However, the features of the resonance data in Fig. 4 were more robust against the decoherence as it probed the initial rise of particle production.

We included the decoherence into the model phenomenologically by implementing a damping term characterized by $\gamma/2\pi = 3.54(94)$ Hz, which was determined by an exponential envelope fit to the data of Fig. 3B. Physically, the damping had several origins: quantum fluctuations; fluctuations of initial state preparation, as well as values of parameters; atom loss; and the spatial dynamics of the two species within the building block. In particular, the first two did not compromise gauge invariance. The last two sources of dissipation can in general be controlled by reducing the particle density and by implementing a deep optical lattice that freezes out the spatial dynamics within individual wells. Fixing γ, the best agreement (solid red line) with the data in Fig. 4A was obtained for $\chi/2\pi = 8.802(8)$ mHz, $\lambda/2\pi = 16.4(6)\mu$Hz, $\Delta_0/2\pi = -4.8(16)$Hz, and $\Delta_L/2\pi = 2.681(1)$kHz. The prediction with these model parameters showed excellent agreement with the data in Fig. 3B (red line) for all times observed. Notably, our established model also described the data in Fig. 4, B to D, by including $\Delta_B/2\pi = -519.3(3)$Hz (see SM). Compared to the ab initio estimates, all fitted values had the expected sign and lie in the same order of magnitude.

Our results demonstrated the controlled operation of an elementary building block of a U(1) gauge theory and thus open the door for large-scale implementations of lattice gauge theories in atomic mixtures. The potential for scalability is an important ingredient for realistic applications to gauge field theory problems. Digital quantum simulations of gauge theories on universal quantum computers (*5*, *9*) are challenging to scale up. This difficulty makes analog quantum simulators, as treated here, highly attractive, because they can be scaled up and still maintain excellent quantum coherence (*6*–*8*, *32*–*34*). Proceeding to the extended system requires optical lattices and Raman-assisted tunneling [see SM and (*22*)]. The resulting extended gauge theory will enable the observation of relevant phenomena, such as plasma oscillations or resonant particle production in strong-field quantum electrodynamics (*35*). Along the path to the relativistic gauge theories realized in nature, we will replace bosonic ^{7}Li with fermionic ^{6}Li, which will allow for the recovery of Lorentz invariance in the continuum limit (see SM).

REFERENCES AND NOTES

1. S. Weinberg, *The Quantum Theory of Fields* (Cambridge Univ. Press, 1995).
2. U.-J. Wiese, *Ann. Phys.* **525**, 777–796 (2013).
3. E. Zohar, J. I. Cirac, B. Reznik, *Rep. Prog. Phys.* **79**, 014401 (2016).
4. M. Dalmonte, S. Montangero, *Contemp. Phys.* **57**, 388–412 (2016).
5. E. A. Martinez *et al.*, *Nature* **534**, 516–519 (2016).
6. C. Kokail *et al.*, *Nature* **569**, 355–360 (2019).
7. H. Bernien *et al.*, *Nature* **551**, 579–584 (2017).
8. F. M. Surace *et al.*, Lattice gauge theories and string dynamics in Rydberg atom quantum simulators. arXiv:1902.09551 [cond-mat.quant-gas] (2019).
9. N. Klco *et al.*, *Phys. Rev. A* **98**, 032331 (2018).
10. L. W. Clark *et al.*, *Phys. Rev. Lett.* **121**, 030402 (2018).
11. F. Görg *et al.*, *Nat. Phys.* **15**, 1161–1167 (2019).
12. C. Schweizer *et al.*, *Nat. Phys.* **15**, 1168–1173 (2019).
13. N. Goldman, G. Juzeliūnas, P. Öhberg, I. B. Spielman, *Rep. Prog. Phys.* **77**, 126401 (2014).
14. F. Chevy, C. Mora, *Rep. Prog. Phys.* **73**, 112401 (2010).
15. F. Grusdt, E. Demler, in *Quantum Matter at Ultralow Temperatures* (Società Italiana di Fisica, 2016), p. 325.
16. T. Rentrop *et al.*, *Phys. Rev. X* **6**, 041041 (2016).
17. D. M. Stamper-Kurn, M. Ueda, *Rev. Mod. Phys.* **85**, 1191–1244 (2013).
18. E. Zohar, J. I. Cirac, B. Reznik, *Phys. Rev. A* **88**, 023617 (2013).
19. K. Stannigel *et al.*, *Phys. Rev. Lett.* **112**, 120406 (2014).
20. V. Kasper, F. Hebenstreit, M. K. Oberthaler, J. Berges, *Phys. Lett. B* **760**, 742–746 (2016).
21. T. V. Zache *et al.*, *Quantum Sci. Technol.* **3**, 034010 (2018).
22. M. E. Tai *et al.*, *Nature* **546**, 519–523 (2017).
23. J. B. Kogut, *Rev. Mod. Phys.* **51**, 659–713 (1979).
24. D. Horn, *Phys. Lett. B* **100**, 149–151 (1981).
25. S. Chandrasekharan, U. J. Wiese, *Nucl. Phys. B* **492**, 455–471 (1997).
26. D. Banerjee *et al.*, *Phys. Rev. Lett.* **109**, 175302 (2012).
27. C. Gross, T. Zibold, E. Nicklas, J. Estève, M. K. Oberthaler, *Nature* **464**, 1165–1169 (2010).
28. M. F. Riedel *et al.*, *Nature* **464**, 1170–1173 (2010).
29. X. Li *et al.*, *Phys. Rev. Lett.* **114**, 255301 (2015).
30. All uncertainties given in this manuscript correspond to a 68% confidence interval for the statistical uncertainty.
31. E. Nicklas *et al.*, *Phys. Rev. Lett.* **107**, 193001 (2011).
32. I. Bloch, J. Dalibard, W. Zwerger, *Rev. Mod. Phys.* **80**, 885–964 (2008).
33. J. I. Cirac, P. Zoller, *Nat. Phys.* **8**, 264–266 (2012).
34. J. Berges, *Nature* **569**, 339–340 (2019).
35. V. Kasper, F. Hebenstreit, J. Berges, *Phys. Rev. D Part. Fields Gravit. Cosmol.* **90**, 025016 (2014).
36. F. Jendrzejewski *et al.*, Realizing a scalable building block of a U(1) gauge theory with cold atomic mixtures, Dryad (2020); https://doi.org/10.5061/dryad.8gtht76k2.

ACKNOWLEDGMENTS

Funding: We acknowledge funding from the DFG Collaborative Research Centre "SFB 1225 (ISOQUANT)," the ERC Advanced Grant "EntangleGen" (Project-ID 694561), the ERC Starting Grant "StrEnQTh" (Project-ID 804305), and the Excellence Initiative of the German federal government and the state governments - funding line Institutional Strategy (Zukunftskonzept): DFG project number ZUK 49/Ü. F.J. acknowledges the DFG support through the project FOR 2724, the Emmy-Noether grant (project-id 377616843) and from the Juniorprofessorenprogramm Baden-Württemberg (MWK). P.H. acknowledges support by Provincia Autonoma di Trento, Quantum Science and Technology in Trento. **Author contributions:** A.M., A.H., A.X. and R.P.B. set up the experiment and performed the measurements; A.M. and T.V.Z. performed the data analysis; T.V.Z., P.H., and J.B. developed the theory; P.H., J.B., M.K.O., and F.J. supervised the project; all authors took part in writing the manuscript. **Competing Interests:** The authors declare no competing interests. **Data and materials availability:** The data are available on the Dryad database (*36*).

SUPPLEMENTARY MATERIALS

science.sciencemag.org/content/367/6482/1128/suppl/DC1
Materials and Methods
Supplementary Text
References (*37*–*42*)

17 September 2019; accepted 4 February 2020
10.1126/science.aaz5312

Science

A scalable realization of local U(1) gauge invariance in cold atomic mixtures

Alexander Mil, Torsten V. Zache, Apoorva Hegde, Andy Xia, Rohit P. Bhatt, Markus K. Oberthaler, Philipp Hauke, Jürgen Berges and Fred Jendrzejewski

Science **367** (6482), 1128-1130.
DOI: 10.1126/science.aaz5312

Gauge invariance with cold atoms

There is considerable interest in developing quantum computational technologies that can simulate a series of physical phenomena inaccessible by classical computers. Mil *et al.* propose a modular scheme for quantum simulation of a U(1) lattice gauge theory based on heteronuclear spin-changing collisions in a mixture of two bosonic quantum gases isolated in single wells of a one-dimensional optical lattice. They engineered the elementary building block for a single well and demonstrate its reliable operation that preserves the gauge invariance. The potential for scalability of the proposed scheme opens up opportunities to address challenges in quantum simulating the continuum limit of the gauge theories.

Science, this issue p. 1128

Science (print ISSN 0036-8075; online ISSN 1095-9203) is published by the American Association for the Advancement of Science, 1200 New York Avenue NW, Washington, DC 20005. The title *Science* is a registered trademark of AAAS.